Journal of Molecular Structure 1260 (2022) 132827

Contents lists available at ScienceDirect

Journal of Molecular Structure

journal homepage: www.elsevier.com/locate/molstr

Integration of catalyst and nucleophile in oxometal aminobis(phenolate) complexes with ammonium iodide pendant arm groups

Anssi Peuronen, Esko Salojärvi, Pasi Salonen, Ari Lehtonen*

Intelligent Materials Chemistry research group, Department of Chemistry, University of Turku, Turku FI-20014, Finland

ARTICLE INFO

Article history:
Received 5 January 2022
Revised 7 March 2022
Accepted 12 March 2022
Available online 15 March 2022

Keywords:
Vanadium
Molybdenum
Uranium
Carbon dioxide
Catalysis
Cyclic carbonate

ABSTRACT

An amine bisphenol ligand with an ammonium iodide group in the pendant arm (H_2L) reacts with V, Mo and U oxometal precursors to form oxovanadium(V), dioxomolybdenum(VI) and dioxouranium(VI) species, respectively. In methanol solutions, vanadium(V) and molybdenum(VI) form 1:1 complexes $[VO(OMe)(L)]I{\cdot}2MeOH$ and $[MoO_2(L)(H_2O)]I{\cdot}2MeOH$, where the cationic charge in the pendant arm is counterbalanced by an iodide anion. Uranium(VI) forms a complex in which the anionic charge of uranate complex unit is compensated by the cationic pendant arm. The complex crystallises as a co-crystal containing a neutral ligand precursor, namely $[UO_2(L)(OAc)]{\cdot}[H_2L]I{\cdot}4MeOH$. The oxovanadium(V) complex combines a Lewis acid, i.e. a pentacoordinated metal centre with a Lewis basic iodide moiety, which makes it a suitable catalyst for the coupling of CO_2 with styrene oxide. The role of the ammonium moiety of the ligand is to carry the iodide nucleophile in the reaction.

1. Introduction

The increase in atmospheric CO_2 level has created a foremost environmental concern, as it is known to participate in the global climate change [1]. Sustainable solutions for the decreasing of atmospheric CO_2 requires the use of fossil-free energy sources as well the development of new chemical technologies that can convert CO_2 to useful chemicals, preferably with economic value [2–8]. For example, the catalytic coupling of CO_2 with epoxides to form cyclic carbonates (Scheme 1) has attracted considerable interest, especially due to its 100% atom economy. As a result a wide range of such catalytic systems have been developed [9].

The active homogeneous systems include various metal-organic catalysts [10–19] as well as some organocatalysts [20–26]. The catalytic coupling reaction with metal-based catalysts follows several steps: (i) the activation of the epoxide by Lewis acidic metal upon coordination through the oxygen atom, (ii) epoxide ring opening by a nucleophile and concomitant formation of a M-OR bond, (iii) the insertion of CO_2 into the metal-alkoxide bond and formation of the organic carbonate by cyclization, which is finally followed by (iv) the release of the cycloaddition products. In general, the catalytic performance of coupling catalysts is based on the cooperation of a Lewis acid centre with a nucleophile, *e.g.* a halide ion. For example, Miceli et al. have used vanadium(V) aminotriphenolate complexes with an Bu_4NI co-catalyst as archetypal examples on highly active catalyst system for the coupling of terminal and internal epoxides with CO_2 [10]. Several two-component organocatalysts based on phenols and Bu_4NX (X = Br, I) have also been shown to couple CO_2 and epoxides efficiently [27–29]. Recently, Hong et al. synthesized an amine bisphenol carrying a quaternary ammonium/iodide ion pair in a pendant arm (Scheme 2), and used it as a single-component organocatalyst for the coupling reaction of propylene oxide with CO_2 [26].

We have previously used amine bisphenol ligands [30] to prepare high oxidation state metal complexes as bio-inspired model compounds and catalysts *e.g.* for epoxidation of alkenes [31–35]. Here we report the use of ammonium-functionalised amine bisphenol to prepare oxovanadium(V), dioxomolybdenum(VI) and dioxouranium(VI) complexes, which carry a cationic group in the ligand pendant arm with the aim of preparing active single-component catalysts that combine Lewis acidic metal centres and a nucleophile part necessary for the coupling reaction. The vanadium complex was studied as a catalyst for the coupling of CO_2 with styrene oxide.

* Corresponding author.
E-mail address: ari.lehtonen@utu.fi (A. Lehtonen).

https://doi.org/10.1016/j.molstruc.2022.132827

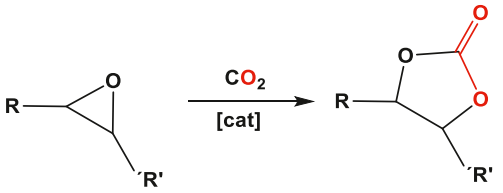

Scheme 1. Coupling of CO_2 with epoxides.

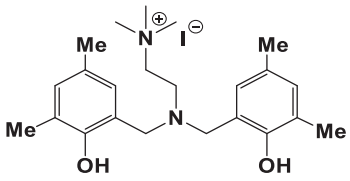

Scheme 2. An organocatalyst for the coupling of CO_2 with epoxides [26].

2. Results and discussions

2.1. Syntheses

The ligand precursor $[H_2L]I$ was prepared by the reaction between a tripodal amine bisphenol and iodomethane in acetonitrile applying a known procedure for corresponding compounds [26]. The reactions of $[H_2L]I$ and metal precursors VO(O-*i*-Pr)$_3$, $MoO_2(acac)_2$ and $UO_2(OAc)_2{\cdot}H_2O$ in methanol lead to the precipitation of the oxometal species $[VO(OMe)(L)]I{\cdot}2MeOH$ (**1**), $[MoO_2(L)(H_2O)]{\cdot}2MeOH$ (**2**) and $[UO_2(L)(OAc)]{\cdot}[H_2L]I{\cdot}4MeOH$ (**3**), respectively (Scheme 3). Vanadium complex **1** crystallized as dark brown needles in a 63% yield. The solid compound is moderately stable under dry air, however, the crystals slowly deteriorate if kept in open atmosphere due to the loss of the solvate molecules. **1** is stable in dry organic solvents, but degrades gradually if wet solvents are used. The ^{1}H NMR spectrum in $CDCl_3$ indicates the presence of few isomers or conformations, as typical for pentacoordinated oxovanadium(V) aminophenolates in non-coordinating solvents [32,36]. However, in MeOH-d_4, one major component (> 99%) is present in the ^{1}H and ^{51}V spectra. The ^{1}H and ^{13}C NMR spectra show anticipated chemical shifts for the deprotonated tridentate ligand. Interestingly, the methoxide ligand is not visible in the spectrum, probably due to the rapid interchange by deuterated solvent. Principally, phenols may act as redox-active, non-innocent ligands through the formation of phenyl radicals upon coordination. For **1**, the ^{51}V chemical shift, -470 ppm, is within the expected range for an oxidation state V(v), which indicates a redox-inactive behaviour [37]. The V=O stretch in the IR spectrum is seen at 948 cm^{-1}, as characteristic for oxovanadium(V) aminophenolates [38].

Complex **2** precipitated from the reaction mixtures as yellow plates, contaminated with some amount of solid impurities. The crystals as well as the contamination were moderately soluble in DMSO but practically insoluble in any other common solvents and therefore **2** could not be purified by washing or recrystallization. The IR spectrum show the $\nu(MoO_2)_s$ and $\nu(MoO_2)_a$ for *cis*-MoO_2 as strong peaks at 914 and 900 cm^{-1} [39]. The ^{1}H and ^{13}C NMR spectra of the crude product comprise typical chemical shifts for the tridentate amine bisphenolate ligand, e.g. benzylic methylene protons are seen as two two-proton doublets at 4.33 and 3.43 ppm, respectively. Similarly, **3** crystallised as brown crystals with some solid impurities and could not be further purified. The NMR spectra in DMSO-d_6 show for coordinated amine bisphenolate ligand show chemical shifts ascribed for the coordinated ligand, e.g. doublets for the benzylic methylene protons at 5.02 and 4.00 ppm, as well as the for the free amine bisphenol molecule. In the IR spectrum, a strong peak was observed at 865 cm^{-1} due to $\nu(UO_2)$, as typical for the presence of a linear O=U=O group [40]. In addition, compounds **2** and **3** were successfully characterized by single-crystal XRD determination of selected crystals.

2.2. Molecular and crystal structures

In the solid state, **1** is formed of ion pairs, which crystallize with two molecules of solvate methanol in the asymmetric unit. In the complex part, the central V(V) ion is coordinated to the tridentate dianionic amine bisphenolate, one oxide anion and one methoxide to form a trigonal bipyramidal coordination sphere. Two phenolate oxygen atoms and an oxo ligand occupy the basal coordination sites while the nitrogen atom in the ligand backbone and a monodentate methoxide group occupy apical positions. The vanadium ion is located slightly above the plane formed by the O atoms. The V–$O_{phenolate}$ distances are 1.829(2) and 1.825(2) Å, respectively, whereas the V–$O_{methoxide}$ distance, 1.788(2) Å, is noticeably shorter. The V–N bond in a trans position to the methoxide ligand is rather long, 2.303(3) Å. The terminal V=O bond length is 1.585(2) Å. In general, the structure and the coordination sphere around the metal centre are typical for the

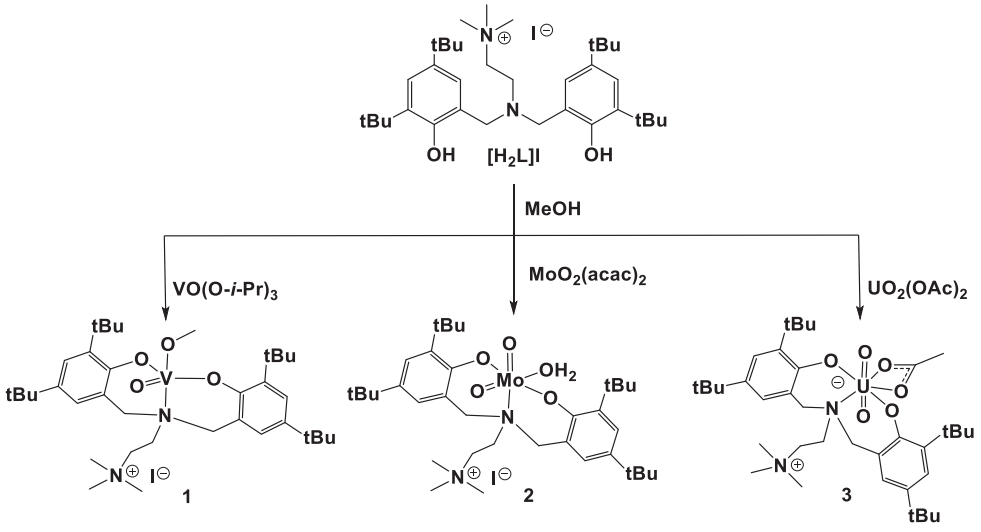

Scheme 3. Preparation of complexes **1**-**3**.

pentacoordinated amine bisphenolate V complexes [36,38,41,42]. The positive charge of the complex unit is located in the pendant ammonium cation, whereas the iodide anion and the solvent molecules are positioned in the cavities of the crystal lattice.

In complex **2**, the amine bisphenolate is coordinated to the dioxomolybdenum(VI) ion as a tridentate ligand through two phenolate oxygen atoms and the nitrogen donor in the ligand backbone. A water molecule is coordinated trans to the oxo group to complete the distorted octahedral coordination sphere. Two terminal oxides, two monoanionic phenolate groups and two neutral donors form a typical *cis*-oxo,*trans*-X,*cis*-L configuration around the metal centre [43]. The O=Mo=O angle, 103.8(2)°, the $O_{phenolate}$–Mo–$O_{phenolate}$ angle, 152.8°, and the Mo=O distances, 1.687(5) and 1.715(4) Å, respectively, are typical for cis-dioxomolybdenum(VI) complexes with tridentate amine bisphenolate ligands [44,45]. The Mo-$O_{phenolate}$ distances are 1.940(4) and 1.930(4) Å, whereas the Mo-N and Mo-O_{water} distances, *i.e.* the bond lengths to the neutral donors, are 2.493(5) and 2.275(5) Å, correspondingly. Again, the positive charge of the complex is located in the pendant-arm ammonium cation while the iodide anion and two solvent molecules reside in the crystal lattice.

Compound **3** is a zwitterion where the anionic charge of the complex unit, formally the uranate anion, is balanced with the cationic charge in the pendant ammonium group. It crystallizes together with one ion pair of $[H_2L]I$ and four methanol molecules. The acetate anion is coordinated as the bidentate ligand and amine bisphenolate in a tridentate manner to the linear dioxouranium(VI) ion, which generates a distorted pentagonal bipyramidal geometry around the metal centre. The O=U=O angle is 179.2° and the U=O bonds are 1.792(3) and 1.790(3) Å, respectively. The U–$O_{phenolate}$ distances are 2.208(4) and 2.196(4) Å, while the U–$O_{acetate}$ distances are noticeably longer, 2.464(4) and 2.483(4) Å, respectively. The U–N distance is also rather long, namely 2.642(4) Å. The overall structure and the geometrical parameters of the complex unit resemble those found previously for $UO_2(HL')(NO_3)]\cdot 2CH_3CN$ (H_2L' = (N,N-bis(2-hydroxy-3,5-dialkylbenzyl)-N′,N′-dimethylethylenediamine; alkyl = Me or tBu) [46].

In all complexes, the tridentate ligand coordinates as an O,N,O donor to form two six-membered chelate rings, though the ligand conformation varies in different compounds. In pentacoordinated **1**, the chelate rings have adopted half-chair conformations. The O1-V1-N8 and O2-V1-N8 bite angles are 79.4 and 79.8°, respectively, whereas the bite distances O1···N8 and O2···N8 are 2.665(4) and 2.673(4) Å. In the six-membered rings, the dihedral angle between the facing bonds O1-C1 and C7-N8 is 33.5°, whereas the dihedral angle between O2–C15 and N8-C12 is -28.1°. The related bite angles in hexacoordinated **2** are of same magnitude, 81.0 and 79.2° as in **1**, while the bite distances are longer, 2.910(6) and 2.853(7) Å, as a result of the longer metal-donor distances. The dihedral angles O1-C1···C7-N8 and O2-C15···N8-C9 are remarkably larger than in **1**, *i.e.* 52.2 and -51.3°, showing more puckered rings. The structures of the chelate rings bear resemblance to boat conformation. In heptacoordinated **3**, the bite angles, 70.4 and 75.1°, are remarkably smaller than in **1** and **2** due to the larger central atom and longer metal-donor bonds. The bite distances, 2.818(6) and 2.968(5) Å, are shorter compared to those in **2**. Similarly to **1**, the conformation of the chelate rings can be described as a half-chair.

2.3. Catalyst studies

As vanadium complex **1** carries a Lewis acid centre and a nucleophilic iodide in a single, isolated compound, it presents as a potential catalyst for the coupling of CO_2 with styrene oxide. In our reaction setup, 0.01 mmol of catalyst sample was mixed with 7 mmol of styrene oxide in an open vial and the reaction mixture was kept in an autoclave at 80 °C for five hours under a CO_2 pressure of 10 bar. The reaction mixtures were subsequently analysed by ^{1}H NMR (Table 4). Along with **1**, the ammonium iodide proligand $[H_2L]I$ as well as the known oxovanadium(V) complex [VO(OMe)(L')] (H_2L' is *N,N′*-bis(2-hydroxy-3,5-di-*tert*-butylbenzyl)-*N′,N′*-dimethylethylene-1,2-diamine), a neutral analogue of **1** [47], were tested as references. A stoichiometric mixture of precursors $[H_2L]I$ and $VO(OPr)_3$ was also tested as an in situ prepared analogue for **1.** Under applied reaction conditions, compound **1** gave styrene carbonate in a 26% yield, the turn-over number (TON) being 182. Interestingly, the free proligand $[H_2L]I$, isolated vanadium compound **1** and the $VO(OPr)_3/[H_2L]I$ mixture gave all styrene carbonate in practically similar yields of which the in situ prepared catalyst displayed highest activity. On the contrary, [VO(OMe)(L')] did not show any catalytic activity in the absence of an additional nucleophile, but it could be activated by a Bu_4NI co-catalyst. On the other hand, it is noteworthy that [VO(OMe)(L')] is hexacoordinated in the solid state, so the activation may require the dissociation of the pendant side-arm donor.

We may suppose that the reactions catalysed by different catalyst systems apply different reaction mechanisms, as well. Specifically, the reaction involving $[H_2L]I$ as a catalyst most likely follows the organocatalytic mechanism proposed by Hong and coworkers [26]. In this reaction mechanism, a phenolic hydrogen bond donor activates the epoxide at the alpha carbon, then iodide nucleophile attacks leading to the formation of the ring-opened alkoxide intermediate. This intermediate subsequently reacts by a CO_2 insertion leading finally to the formation of a cyclic product [26]. Conversely, complex **1** as well as the two-component systems $VO(OPr)_3/[H_2L]I$ and $[VO(OMe)(L')]/Bu_4NI$ follow apparently the mechanism proposed by Licini and co-workers for the oxovanadium(v)aminotrisphenolate/ammoniumiodide system. In the suggested mechanism, the coordination of the epoxide to the metal through the oxygen donor is followed by either an internal (by the alkoxide/phenoxide oxygen) or an external (by the halide) nucleophilic attack, a CO_2 insertion and a final cyclisation [10]. As [VO(OMe)(L')] did not show any activity without an external nucleophile, the internal nucleophiles, *i.e.* phenolate oxygens or coordinated nitrogen donor seem not to participate the reaction.

In conclusion, an ammonium iodide -functionalised amine bisphenol reacts with V, Mo and U precursors as a tridentate O,N,O donor to form mononuclear oxovanadium(V), dioxomolybdenum(VI) and dioxouranium(VI) species, respectively. In the oxovanadium(V) and dioxomolybdenum(VI) complexes, the cationic charge in the pendant arm is balanced by iodide counter ion. By contrast, uranyl cation forms a zwitterionic complex, in which the anionic charge of uranate complex unit is compensated by the cationic pendant arm of the ligand. The oxovanadium(V) complex combines a Lewis acid metal centre and Lewis basic iodide moiety, which makes it the catalyst for the coupling of CO_2 with styrene oxide. Study of the catalytic activity of the vanadium complex provided evidence on the importance of the ammonium moiety of the ligand since it serves the role of carrying the iodide nucleophile in the reaction.

3. Experimental

All syntheses and manipulations were carried out under ambient atmosphere. The solvents and chemicals purchased from commercial suppliers were used without further purifications. The IR spectra were measured with Bruker Optics, Vertex 70 device with a diamond ATR setup, whereas the NMR spectra were recorded with Bruker Avance 500 NMR (^{1}H: 500 MHz, ^{51}V: 132 MHz, ^{13}C: 125 MHz) NMR spectrometer at 25 °C (298 K). The spectrometer was equipped with a broad-band observe probe (Bruker BBO-5 mm-Zgrad). The 0 ppm vanadium reference frequency was cal-

culated from the TMS ^{1}H frequency using the unified chemical shift scale by IUPAC ($\Xi(^{51}V, VOCl_3) = 26.302948$) [48]. Complex [VO(OMe)(L')] was prepared as previously reported [47]. The NMR spectra are given in

3.1. [H_2L]I

The ligand precursor was made applying a known procedure for corresponding compounds [26] 2.1 g (4 mmol) of *N,N′*-bis(2-hydroxy-3,5-di-*tert*-butylbenzyl)-*N′,N′*-dimethylethylene-1,2-diamine [47] and 1.4 g of MeI (10 mmol) were mixed in 20 ml of acetonitrile and heated to the reflux temperature for three hours. The reaction mixture was allowed to cool to room temperature and 2.1 g (78%) of [H_2L]I was isolated by filtration, washed with cold acetonitrile and dried in vacuum. ^{1}H NMR ($CDCl_3$): δ 7.43 (s, 2H, Ar*OH*), 7.26 (d, J = 2.2 Hz, 2H, ArH), 6.99 (d, J = 2.1 Hz, 2H, ArH.), 3.98 (t, J = 6.3 Hz, 2H, *CH*$_2$NMe$_3$), 3.83 (s, 4H, Ar*CH*$_2$), 3.22 (s, 9H, N*Me*$_3$), 3.00 (t, J = 6.2 Hz, 2H, N*CH*$_2$), 1.41 (s, 18H, *t*-Bu), 1.29 (s, 18H, *t*-Bu).

3.2. [VO(OMe)(L)]I·2 MeOH (1)

134 mg (0.20 mmol) of [H_2L]I was dissolved in 4 ml of MeOH and 50 µl (0.20 mmol) of $VO(OPr)_3$ was added. The dark solution was kept at +4 °C for three days to obtain 105 mg (63%) of **1** as dark brown needles. A sample was kept in a vacuum desiccator for two days prior to the elemental and spectral analyses to remove the possible non-stoichiometric amount of the solvent of crystallisation. Found: C: 56.54; H: 7.81; N: 3.68. Calcd. for $C_{36}H_{60}IN_2O_4V$: C: 56.69; H: 7.93; N: 3.67. IR (cm^{-1}) 2954w, 1438w, 1236m, 1168w, 1054s, 989w, 948m (V=O), 914m, 852m, 806w, 757m, 595s, 549w, 476w, 368w. ESI(+)-MS: *m/z* 635.4062 ([VO(OMe)(L)]$^+$ calcd. *m/z* 635.3993). UV-Vis: 285 nm (ε = 25 500 $M^{-1}cm^{-1}$), 360 nm (ε = 10 500 $M^{-1}cm^{-1}$). ^{1}H NMR (MeOH-d_4): δ 7.39 (d, J = 2.2 Hz, 2H, ArH), 7.30 (d, J = 2.2 Hz, 2H, ArH), 4.29 (d, J = 12.7 Hz, 2H, Ar*CH*$_2$), 3.64 (m, 2H, N*CH*$_2$), 3.54 (d, J = 12.7 Hz, 2H, Ar*CH*$_2$), 3.12 (m, 2H, N*CH*$_2$), 2.84 (s, 9H, N*Me*$_3$), 1.55 (s, 18H, t-Bu), 1.34 (s, 18H, t-Bu). ^{51}V NMR (MeOH-d_4): -470 (major component, > 90%), -532 (minor), -553 (minor). ^{13}C NMR (MeOH-d_4): 165.4, 143.1, 137.2, 125.2, 125.1, 123.8, 60.4, 58.0, 54.2, 45.3, 36.3, 35.4, 32.3, 31.4.

3.3. [MoO_2(L)]I·2 MeOH (2)

134 mg (0.20 mmol) of [H_2L]I was dissolved in 4 ml of MeOH and 65 mg (0.20 mmol) of $MoO_2(acac)_2$ was added. The solution was kept at room temperature for three days to obtain 120 mg of **2** as yellow crystals together with a small amount colourless precipitate. The crystalline material is poorly soluble in common solvents and was not further purified. IR: 3421w(br), 3280w, 2958m, 2904m, 2869w, 1475vs, 1443m, 1413s, 1388m, 1360m, 1303m, 1254s, 1236s, 1203s, 1169s, 1128s, 1099w, 1022m, 1016s, 991w, 970w, 940s, 914s, 900vs, 843vs, 808w, 783w, 754s, 653w, 600w, 569s, 555s, 499m, 478m cm^{-1}. ^{1}H NMR (DMSO-d_6,): δ 7.46 (d, J = 2.2, 2H, Ar*H*), 7.24 (d, J = 2.2 Hz, 2H, Ar*H*), 4.33 (d, 2H, J = 11.5 Hz, Ar*CH*$_2$), 4.09 (q, J = 5.5 Hz, 2H, CH_3*OH*), 3.64 (m, 2H, *CH*$_2$NMe$_3$), 3.43 (d, 2H, J = 11.5 Hz, Ar*CH*$_2$), 3.18 (d, J = 5Hz, 6H, *CH*$_3$OH), 2.91 (m, 2H, N*CH*$_2$), 2.78, (s, 9H, N*Me*$_3$), 1.39 (s, 18H, t-Bu), 1.29 (s, 18H, t-Bu). ^{13}C NMR (DMSO-d_6): 159.7, 141.7, 135.8, 125.3, 123.4, 123.1, 55.0, 52.8, 48.6, 34.65, 34.2, 31.6, 30.1.

3.4. [UO_2(L)(OAc)]·[H_2L]I·4MeOH (3)

67 mg (0.10 mmol) of [H_2L]I was dissolved in 3 ml of MeOH and 42 mg (0.10 mmol) of $UO_2(CH_3COO)_2{\cdot}2H_2O$ was added. The solution was kept at room temperature for three days to obtain 60 mg of **3** as brown crystals. The product contained a small amount of slightly coloured microcrystals, whereas attempts to purify the sample by washing or recrystallization failed. IR: 3344w(br), 2953m, 2906m, 2862m, 1543m, 1477vs, 1445vs, 1414s, 1387m, 1360m, 1308s, 1284m, 1271s, 1238s, 1205s, 1167m, 1130m, 1109m, 1049w, 989w, 969w, 914m, 865vs, 837s, 806m, 785m, 770m, 744m, 673m, 648m, 619s, 602s, 526s cm^{-1}. ^{1}H NMR (DMSO-d_6): δ 9.00 (s, 2H, Ar*OH*), 7.36 (s, 2H, Ar*H*), 7.34 (s, 2H, Ar*H*), 7.15 (s, 2H, Ar*H*), 7.04 (2H, Ar*H*), 5.01 (d, 2H, J = 12.3 Hz, Ar*CH*$_2$), 4.00 (d, 2H, J = 12.3 Hz, Ar*CH*$_2$), 3.75 (s, 4H, Ar*CH*$_2$), 3.53 (t, J = 6.3 Hz, 2H, *CH*$_2$NMe$_3$), 3.44 (m, 2H, *CH*$_2$NMe$_3$), 3.25 (m, 2H, N*CH*$_2$), 2.92 (s, 9H, N*Me*$_3$), 2.85 (t, J = 6.3 Hz, 2H, N*CH*$_2$), 2.53 (s, 9H, N*Me*$_3$), 2.33 (s, 3H, OAc), 1.68 (s, 18H, t-Bu), 1.36 (s, 18H, t-Bu), 1.32 (s, 18H, t-Bu), 1.24 (s, 18H, t-Bu). ^{13}C NMR (DMSO-d_6): 184.3, 166.2, 152.4, 141.0, 137.4, 136.8, 136.2, 125.0, 124.9, 124.8, 123.0, 122.6, 122.5, 61.2, 61.0, 60.4, 54.5, 52.4, 52.3, 45.0, 42.6, 34.8, 34.6, 33.9, 33.6, 32.0, 31.4, 30.3, 29.6.

Table 1
Selected distances (Å) and angles (°) in **1.**

V1-O1	1.829(2)	O1-V1-O2	127.46(11)
V1-O2	1.825(2)	O1-V1-O3	113.34(11)
V1-O3	1.585(2)	O2-V1-O3	113.03(11)
V1-O4	1.788(2)	O3-V1-O4	100.92(12)
V1-N8	2.303(3)	O1-V1-N8	79.41(10)
N18···I1	4.357(3)	O2-V1-N8	79.80(10)
O1···N8	2.665(4)	O3-V1-N8	86.90(13)
O2···N8	2.673(4)	O4-V1-N8	172.22(11)

Table 2
Selected bond lengths (Å) and angles (°) in **2.**

Mo1-O1	1.940(4)	O1-Mo1-O2	152.80(19)
Mo1-O2	1.930(5)	O3-Mo1-O4	103.8(2)
Mo1-O3	1.687(5)	O3-Mo1-O5	164.9(2)
Mo1-O4	1.715(4)	O4-Mo1-O5	91.28(19)
Mo1-O5	2.275(5)	O1-Mo1-N8	81.04(18)
Mo1-N8	2.493(5)	O2-Mo1-N8	79.24(18)
N18···I1	4.496(5)	O3-Mo1-N8	86.76(19)
O1···N8	2.910(6)	O4-Mo1-N8	169.44(19)
O2···N8	2.853(7)	O5-Mo1-N8	78.25(16)

Table 3
Selected bond lengths (Å) and angles (°) in **3.**

U1-O1	2.208(4)	O1-U1-O2	145.13(12
U1-O2	2.196(4)	O3-U1-O4	179.15(18)
U1-O3	1.792(3)	O5-U1-O6	52.86(13)
U1-O4	1.790(3)	O1-U1-N8	70.41(13)
U1-O5	2.464(4)	O2-U1-N8	75.06(12)
U1-O6	2.483(4)	O3-U1- N8	94.45(14)
U1-N8	2.642(4)	O4-U1-N8	85.49(13)
O1···N8	2.818(6)	O5-U1-N8	156.88(14)
O2···N8	2.968(5)	O6-U1-N8	149.00(13)

Table 4
Catalytic coupling of CO_2 and styrene oxide.

Catalyst	Yield-% of styrene carbonate[a]	TON
1	26	182
[H_2L]I	24	168
[H_2L]I + $VO(OPr)_3$	30	210
[VO(OMe)(L')]	–	–
[VO(OMe)(L')] + Bu_4NI	19	133
no catalyst	–	–

[a] The yields are mean values of two parallel reactions.

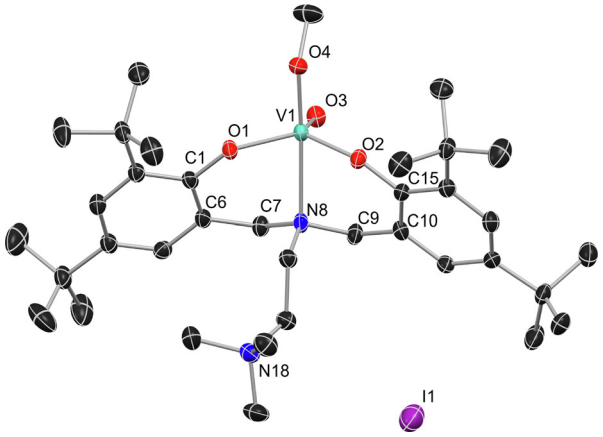

Fig. 1. The molecular structure of [VO(OMe)(L)]I·2 MeOH (1). The H–atoms and the solvent molecules are omitted for the clarity. Displacement ellipsoids shown at the 50% probability level.

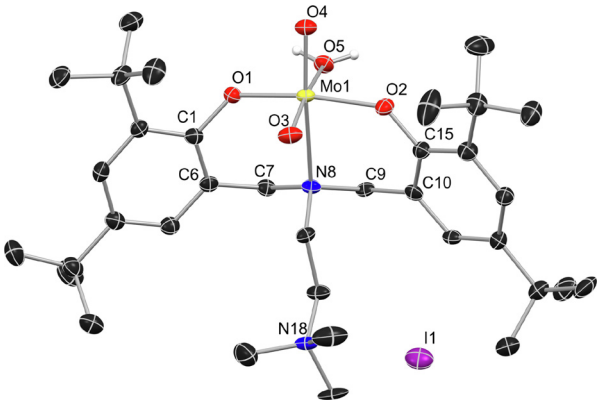

Fig. 2. The molecular structure of [MoO_2(L)]I·2 MeOH (2). The C–H hydrogen atoms and solvent molecules are removed for clarity. Displacement ellipsoids shown at the 50% probability level.

3.5. Catalyst studies

In each experiment, the 0.01 mmol sample of the catalyst (**1**, [H_2L]I, [H_2L]I + VO(OPr)$_3$, [VO(OMe)(L')] or [VO(OMe)(L')] + Bu_4NI) was mixed in 0.8 ml (7 mmol) of styrene oxide and the reaction mixture was put in a stainless steel autoclave. The blank reaction was run without any catalyst. The reactor was then pressurized with CO_2 to 10 bar at 80°C for five hours, whereas the reaction mixtures were subsequently analysed by ^{1}H NMR by comparing the integrated intensities of aliphatic hydrogens in styrene oxide at 5.70, 4.83 and 4.37 ppm, respectively, to those chemical shifts of styrene carbonate at 3.88, 3.17 and 2.84 ppm.

3.6. Single crystal X-ray diffraction

Data were collected on a Bruker-Nonius KappaCCD diffractometer with Apex II detector using Mo K_α radiation and the crystals kept at 170 K during data collection. For data collection, processing, and absorption correction the software packages COLLECT [49], DENZO-SMN [50] and SADABS [51] were, respectively used. The structure solving (direct methods) and refinement on F^2 by full-matrix least-squares techniques were done within Olex2 [52] environment using SHELXS [53] and SHELXL [54] software packages, respectively. All non-hydrogen atoms were refined anisotropically whereas hydrogen atoms were refined using isotropic displacement parameters. O–H hydrogen atoms were located from the difference density map when possible (all phenol groups and water molecules as well as some of the methanol solvent molecules) and refined using O–H distance restraints. The remaining MeOH O–H and all C–H hydrogen atoms were refined with a riding atom model. The final refinement of structure of **2** was carried out using a HKLF5 file consisting of two domains in a ca. 6:4 ratio, which resulted in significant improvement of the refinement (Figs. 1–3, Tables 1–3, Table 5).

Table 5
Crystallographic data for complexes **1**-**3**.

	1	**2**	**3**
Empirical formula	$C_{38}H_{68}IN_2O_6V$	$C_{37}H_{67}IMoN_2O_7$	$C_{75}H_{131}IN_4O_{11}U$
CCDC reference	2132345	2132343	2132344
Formula weight	826.78	874.76	1629.76
Temperature/K	170	170	170
Crystal system	Monoclinic	Triclinic	Monoclinic
Space group	$P2_1/n$	$P\bar{1}$	$P2_1/c$
a/Å	18.5210(6)	10.8785(2)	20.7466(4)
b/Å	10.4999(2)	14.2937(3)	14.5567(2)
c/Å	22.1057(6)	15.1734(3)	28.3301(6)
α/°	90	71.5570(10)	90
β/°	92.7354(10)	77.6973(12)	102.2860(10)
γ/°	90	75.4295(12)	90
Volume/Å^3	4294.0(2)	2143.19(7)	8359.8(3)
Z	4	2	4
ρ_{calc}g/cm^3	1.279	1.356	1.295
μ/mm^{-1}	0.991	1.07	2.364
F(000)	1736	908	3368
Crystal size/mm^3	0.3 × 0.25 × 0.22	0.40 × 0.36 × 0.20	0.50 × 0.35 × 0.30
Radiation	MoKα (λ = 0.71073)	MoKα (λ = 0.71073)	MoKα (λ = 0.71073)
2Θ range for data collection/°	4.404 to 51.998	3.564 to 51.994	3.574 to 52
Index ranges	-13 ≤ h ≤ 22, -12 ≤ k ≤ 12, -27 ≤ l ≤ 26	-13 ≤ h ≤ 13, -17 ≤ k ≤ 17, -12 ≤ l ≤ 18	-25 ≤ h ≤ 21, -17 ≤ k ≤ 14, -33 ≤ l ≤ 34
Reflections collected	22885	8230	41637
Independent reflections	8317 [R_{int} = 0.0375, R_{sigma} = 0.0507]	8230 [R_{sigma} = 0.0584]	16034 [R_{int} = 0.0394, R_{sigma} = 0.0572]
Data/restraints/parameters	8317/0/453	8230/2/464	16034/5/885
Goodness-of-fit on F^2	1.061	1.067	1.094
Final R indexes [I>=2σ (I)]	R_1 = 0.0518, wR_2 = 0.0916	R_1 = 0.0702, wR_2 = 0.1481	R_1 = 0.0495, wR_2 = 0.0872
Final R indexes [all data]	R_1 = 0.0731, wR_2 = 0.1008	R_1 = 0.0797, wR_2 = 0.1530	R_1 = 0.0744, wR_2 = 0.0969
Largest diff. peak/hole / e Å^{-3}	0.60/-0.77	1.26/-1.74	0.90/-0.58

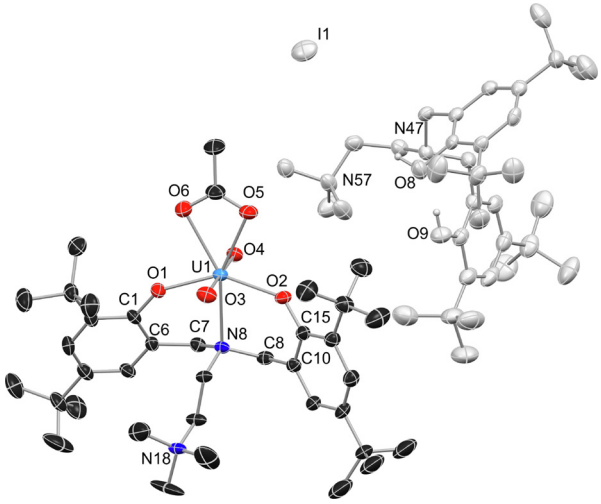

Fig. 3. The molecular structure of the complex unit in $[UO_2(L)(OAc)]\cdot[H_2L]I\cdot 4MeOH$ (3). The C–H hydrogen atoms and solvent molecules are removed for clarity whereas the $[H_2L]I$ ion pair is presented in light grey colour. Displacement ellipsoids shown at the 50% probability level.

Declaration of Competing Interest

The authors declare the following financial interests/personal relationships which may be considered as potential competing interests: Anssi Peuronen reports financial support was provided by Academy of Finland.

CRediT authorship contribution statement

Anssi Peuronen: Investigation, Writing – review & editing. **Ari Lehtonen:** Conceptualization, Supervision, Investigation, Writing – original draft.

Acknowledgements

We greatly acknowledge Mr. Qingan Wang for the number of catalyst tests. This work was supported by Academy of Finland (project no. 315911, for A.P.).

Supplementary materials

Supplementary material associated with this article can be found, in the online version, at doi:10.1016/j.molstruc.2022.132827.

References

[1] T.R. Anderson, E. Hawkins, P.D. Jones, CO_2, the greenhouse effect and global warming: from the pioneering work of Arrhenius and callendar to today's earth system models, Endeavour 40 (2016) 178–187, doi:10.1016/j.endeavour.2016.07.002.
[2] C. Maeda, Y. Miyazaki, T. Ema, Recent progress in catalytic conversions of carbon dioxide, Catal. Sci. Technol. 4 (2014) 1482–1497, doi:10.1039/c3cy00993a.
[3] J. Martínez, F. De La Cruz-Martínez, M.A. Gaona, E. Pinilla-Pealver, J. Fernández-Baeza, A.M. Rodríguez, J.A. Castro-Osma, A. Otero, A. Lara-Sánchez, Influence of the counterion on the synthesis of cyclic carbonates catalyzed by bifunctional aluminum complexes, Inorg. Chem. 58 (2019) 3396–3408, doi:10.1021/acs.inorgchem.8b03475.
[4] F.M. Mota, D.H. Kim, From CO_2 methanation to ambitious long-chain hydrocarbons: alternative fuels paving the path to sustainability, Chem. Soc. Rev. 48 (2019) 205–259, doi:10.1039/c8cs00527c.
[5] Q. Liu, L. Wu, R. Jackstell, M. Beller, Using carbon dioxide as a building block in organic synthesis, Nat. Commun. 6 (2015), doi:10.1038/ncomms6933.
[6] J.N. Appaturi, R.J. Ramalingam, M.K. Gnanamani, G. Periyasami, P. Arunachalam, R. Adnan, F. Adam, M.D. Wasmiah, H.A. Al-Lohedan, Review on carbon dioxide utilization for cycloaddition of epoxides by ionic liquid-modified hybrid catalysts: effect of influential parameters and mechanisms insight, Catalysts 11 (2020) 4, doi:10.3390/catal11010004.
[7] M. Aresta, A. Dibenedetto, A. Angelini, Catalysis for the valorization of exhaust carbon: from CO_2 to chemicals, materials, and fuels. Technological use of CO_2, Chem. Rev. 114 (2014) 1709–1742, doi:10.1021/cr4002758.
[8] J. Artz, T.E. Müller, K. Thenert, J. Kleinekorte, R. Meys, A. Sternberg, A. Bardow, W. Leitner, Sustainable conversion of carbon dioxide: an integrated review of catalysis and life cycle assessment, Chem. Rev. 118 (2018) 434–504, doi:10.1021/acs.chemrev.7b00435.
[9] A. Monfared, R. Mohammadi, A. Hosseinian, S. Sarhandi, P.D. Kheirollahi Nezhad, Cycloaddition of atmospheric CO_2 to epoxides under solvent-free conditions: a straightforward route to carbonates by green chemistry metrics, RSC Adv. 9 (2019) 3884–3899, doi:10.1039/c8ra10233c.
[10] C. Miceli, J. Rintjema, E. Martin, E.C. Escudero-Adán, C. Zonta, G. Licini, A.W. Kleij, Vanadium(V) catalysts with high activity for the coupling of epoxides and CO_2: characterization of a putative catalytic intermediate, ACS Catal. 7 (2017) 2367–2373, doi:10.1021/acscatal.7b00109.
[11] S. Ta, M. Ghosh, R.A. Molla, S. Ghosh, M. Islam, P. Brandão, V. Félix, D. Das, Naphthalene based amide-imine derivative and its dinuclear vanadium complex: structures, atmospheric CO_2 fixation and theoretical support, ChemistrySelect 4 (2019) 10254–10259, doi:10.1002/slct.201901327.
[12] F.Della D. Monica, B. Maity, T. Pehl, A. Buonerba, A. De Nisi, M. Monari, A. Grassi, B. Rieger, L. Cavallo, C. Capacchione, [OSSO]-type iron(III) complexes for the low-pressure reaction of carbon dioxide with epoxides: catalytic activity, reaction kinetics, and computational study, ACS Catal. 8 (2018) 6882–6893, doi:10.1021/acscatal.8b01695.
[13] M. Taherimehr, J.P.C.C. Sertã, A.W. Kleij, C.J. Whiteoak, P.P. Pescarmona, New iron pyridylamino-bis(Phenolate) catalyst for converting CO_2 into cyclic carbonates and cross-linked polycarbonates, ChemSusChem (2015), doi:10.1002/cssc.201403323.
[14] N.H. Kim, E.Y. Seong, J.H. Kim, S.H. Lee, K.-H. Ahn, E.J. Kang, Functionally-designed heteroleptic Fe-bisiminopyridine systems for the transformation of carbon dioxide, J. CO_2 Util. (2019), doi:10.1016/j.jcou.2019.07.033.
[15] Z.A.K. Khattak, H.A. Younus, N. Ahmad, H. Ullah, S. Suleman, M.S. Hossain, M. Elkadi, F. Verpoort, Highly active dinuclear cobalt complexes for solvent-free cycloaddition of CO_2 to epoxides at ambient pressure, Chem. Commun. (2019), doi:10.1039/c9cc02626f.
[16] Y.A. Rulev, V.A. Larionov, A.V. Lokutova, M.A. Moskalenko, O.L. Lependina, V.I. Maleev, M. North, Y.N. Belokon, Chiral cobalt(III) complexes as bifunctional brønsted acid-lewis base catalysts for the preparation of cyclic organic carbonates, ChemSusChem (2016), doi:10.1002/cssc.201501365.
[17] C. Maeda, S. Sasaki, T. Ema, Electronic tuning of zinc porphyrin catalysts for the conversion of epoxides and carbon dioxide into cyclic carbonates, ChemCatChem (2017), doi:10.1002/cctc.201601690.
[18] J.L.S. Milani, W. de Almeida Bezerra, A.K.S.M. Valdo, F.T. Martins, L.T.F. de Melo Camargo, V.H. Carvalho-Silva, S.S. dos Santos, D. Cangussu, R.P. das Chagas, Zinc complexes with 1,2-disubstituted benzimidazole ligands: experimental and theoretical studies in the catalytic cycloaddition of CO_2 with epoxides, Polyhedron (2019), doi:10.1016/j.poly.2019.114134.
[19] X. Wu, M. North, A bimetallic aluminium(salphen) complex for the synthesis of cyclic carbonates from epoxides and carbon dioxide, ChemSusChem (2017), doi:10.1002/cssc.201601131.
[20] Y. Kumatabara, M. Okada, S. Shirakawa, Triethylamine hydroiodide as a simple yet effective bifunctional catalyst for CO_2 fixation reactions with epoxides under mild conditions, ACS Sustain. Chem. Eng. (2017), doi:10.1021/acssuschemeng.7b01535.
[21] J. Steinbauer, C. Kubis, R. Ludwig, T. Werner, Mechanistic study on the addition of CO_2 to epoxides catalyzed by ammonium and phosphonium salts: a combined spectroscopic and kinetic approach, ACS Sustain. Chem. Eng. (2018), doi:10.1021/acssuschemeng.8b02093.
[22] Y. Toda, Y. Komiyama, H. Esaki, K. Fukushima, H. Suga, Methoxy groups increase reactivity of bifunctional tetraarylphosphonium salt catalysts for carbon dioxide fixation : a mechanistic study methoxy groups increase reactivity of bifunctional tetraarylphosphonium salt catalysts for carbon dioxide fixation : a, J. Org. Chem. (2019), doi:10.1021/acs.joc.9b02581.
[23] F.D. Bobbink, D. Vasilyev, M. Hulla, S. Chamam, F. Menoud, G. Laurenczy, S. Katsyuba, P.J. Dyson, Intricacies of cation-anion combinations in imidazolium salt-catalyzed cycloaddition of CO_2 into epoxides, ACS Catal. (2018), doi:10.1021/acscatal.7b04389.
[24] O. Martínez-Ferraté, G. Chacón, F. Bernardi, T. Grehl, P. Brüner, J. Dupont, Cycloaddition of carbon dioxide to epoxides catalysed by supported ionic liquids, Catal. Sci. Technol. (2018), doi:10.1039/c8cy00749g.
[25] X. Wu, C. Chen, Z. Guo, M. North, A.C. Whitwood, Metal- and halide-free catalyst for the synthesis of cyclic carbonates from epoxides and carbon dioxide, ACS Catal. 9 (2019) 1895–1906, doi:10.1021/acscatal.8b04387.
[26] M. Hong, Y. Kim, H. Kim, H.J. Cho, M.H. Baik, Y. Kim, Scorpionate catalysts for coupling CO_2 and epoxides to cyclic carbonates: a rational design approach for organocatalysts, J. Org. Chem. 83 (2018) 9370–9380, doi:10.1021/acs.joc.8b00722.
[27] H. Büttner, K. Lau, A. Spannenberg, T. Werner, Bifunctional one-component catalysts for the addition of carbon dioxide to epoxides, ChemCatChem (2015), doi:10.1002/cctc.201402816.
[28] L. Martínez-Rodríguez, J. Otalora Garmilla, A.W. Kleij, Cavitand-based polyphenols as highly reactive organocatalysts for the coupling of carbon dioxide and oxiranes, ChemSusChem (2016), doi:10.1002/cssc.201501463.
[29] C.J. Whiteoak, A. Nova, F. Maseras, A.W. Kleij, Merging sustainability with organocatalysis in the formation of organic carbonates by using CO_2 as a feedstock, ChemSusChem (2012), doi:10.1002/cssc.201200255.

[30] O. Wichmann, R. Sillanpää, A. Lehtonen, Structural properties and applications of multidentate [O,N,O,X'] aminobisphenolate metal complexes, Coord. Chem. Rev. 256 (2012), doi:10.1016/j.ccr.2011.09.007.
[31] E. Salojärvi, A. Peuronen, R. Sillanpää, P. Damlin, H. Kivelä, A. Lehtonen, Aminobisphenolate supported tungsten disulphido and dithiolene complexes, Dalt. Trans. 44 (2015), doi:10.1039/c5dt00995b.
[32] P. Salonen, A. Peuronen, A. Lehtonen, Oxidovanadium(V) amine bisphenolates as epoxidation, sulfoxidation and catechol oxidation catalysts, Inorg. Chem. Commun. 86 (2017) 165–167, doi:10.1016/j.inoche.2017.10.017.
[33] M.M. Hänninen, A. Peuronen, P. Damlin, V. Tyystjärvi, H. Kivelä, A. Lehtonen, Vanadium complexes with multidentate amine bisphenols, Dalt. Trans. 43 (2014) 14022–14028, doi:10.1039/C4DT01007H.
[34] J.A. Schachner, N.C. Mösch-Zanetti, A. Peuronen, A. Lehtonen, Dioxidomolybdenum(VI) and –tungsten(VI) complexes with tetradentate amino bisphenolates as catalysts for epoxidation, Polyhedron 134 (2017), doi:10.1016/j.poly.2017.06.011.
[35] P. Salonen, R. Savela, A. Peuronen, A. Lehtonen, Vanadium aminophenolates in catechol oxidation: conformity with Finke's common catalyst hypothesis, Dalt. Trans. 50 (2021) 6088–6099, doi:10.1039/d1dt00419k.
[36] C. Lorber, E. Despagnet-Ayoub, L. Vendier, A. Arbaoui, C. Redshaw, Amine influence in vanadium-based ethylene polymerisation pro-catalysts bearing bis(phenolate) ligands with "pendant" arms, Catal. Sci. Technol. (2011), doi:10.1039/c1cy00089f.
[37] C.R. Cornman, J. Kampf, V.L. Pecoraro, Structural and spectroscopic characterization of vanadium(V)-oxoimidazole complexes, Inorg. Chem. 31 (1992) 1981–1983, doi:10.1021/ic00037a001.
[38] M.K. Hossain, M. Haukka, G.C. Lisensky, A. Lehtonen, E. Nordlander, Oxovanadium(V) complexes with tripodal bisphenolate and monophenolate ligands: syntheses, structures and catalytic activities, Inorg. Chim. Acta (2019), doi:10.1016/j.ica.2018.11.049.
[39] A. Peuronen, R. Sillanpää, A. Lehtonen, The syntheses and vibrational spectra of 16O- and 18O-enriched cis-MO2 (M=Mo, W) complexes, Chemistry Select 3 (2018) 3814–3818, doi:10.1002/slct.201800671.
[40] R. Kannappan, S. Tanase, D.M. Tooke, A.L. Spek, I. Mutikainen, U. Turpeinen, J. Reedijk, Separation of actinides and lanthanides: crystal and molecular structures of N,N′-bis(3,5-di-t-butylsalicylidene)-4,5-dimethyl-1,2-phenylenediamine and its uranium complex, Polyhedron 23 (2004) 2285–2291, doi:10.1016/j.poly.2004.07.004.
[41] G. Zhang, B.L. Scott, R. Wu, L.A.P. Silks, S.K. Hanson, Aerobic oxidation reactions catalyzed by vanadium complexes of bis(phenolate) ligands, Inorg. Chem. (2012), doi:10.1021/ic3007525.
[42] D. Maity, J. Marek, W.S. Sheldrick, H. Mayer-Figge, M. Ali, Synthesis, crystal structures and catalytic oxidation of aromatic hydrocarbons by oxovanadium(V) complexes of aminebis(phenolate) ligands, J. Mol. Catal. A Chem. (2007), doi:10.1016/j.molcata.2007.01.041.
[43] G. Barea, A. Lledos, F. Maseras, Y. Jean, Cis,trans,cis or All-cis geometry in d0 octahedral dioxo complexes. An IMOMM study of the role of steric effects, Inorg. Chem. 37 (1998) 3321–3325, doi:10.1021/ic971226e.
[44] A. Riisiö, A. Lehtonen, M.M. Hänninen, R. Sillanpää, Synthesis, structure and catalytic properties of dinuclear Mo^{VI} complexes with ditopic diaminotetraphenols, Eur. J. Inorg. Chem. (2013), doi:10.1002/ejic.201201234.
[45] A. Lehtonen, R. Sillanpää, Dioxomolybdenum(VI) complexes with tri- and tetradentate aminobis(phenolate)s, Polyhedron 24 (2005), doi:10.1016/j.poly.2004.11.003.
[46] H. Sopo, A. Lehtonen, R. Sillanpää, Uranyl(VI) complexes of [O,N,O,N′]-type diaminobis(phenolate) ligands: syntheses, structures and extraction studies, Polyhedron 27 (2008), doi:10.1016/j.poly.2007.08.047.
[47] N. Noshiranzadeh, M. Mayeli, R. Bikas, K. Ślepokura, T. Lis, Selective catalytic oxidation of benzyl alcohol to benzaldehyde by a mononuclear oxovanadium(V) complex of a bis(phenolate) ligand containing bulky tert-butyl substituents, Transit. Met. Chem. 39 (2014) 33–39, doi:10.1007/s11243-013-9769-6.
[48] R.K. Harris, E.D. Becker, S.M.C. De Menezes, R. Goodfellow, P. Granger, NMR nomenclature: nuclear spin properties and conventions for chemical shifts - IUPAC recommendations 2001, Solid State Nucl. Magn. Reson. 22 (2002) 458–483, doi:10.1006/snmr.2002.0063.
[49] R.W.W. Hooft, Nonius, Nonius BV, Delft, The Netherlands, 1998.
[50] Z. Otwinowski, W. Minor, Processing of X-ray diffraction data collected in oscillation mode, Methods Enzymol. 276 (1997) 307–326, doi:10.1016/S0076-6879(97)76066-X.
[51] G.M. Sheldrick, SADABS-2021/1, University of Göttingen, Germany, 1996.
[52] O.V. Dolomanov, L.J. Bourhis, R.J. Gildea, J.A.K. Howard, H. Puschmann, OLEX2: a complete structure solution, refinement and analysis program, J. Appl. Crystallogr. 42 (2009) 339–341, doi:10.1107/S0021889808042726.
[53] G.M. Sheldrick, A short history of SHELX, Acta Crystallogr. Sect. A Found. Crystallogr. 64 (2008) 112–122, doi:10.1107/S0108767307043930.
[54] G.M. Sheldrick, Crystal structure refinement with SHELXL, Acta Crystallogr. Sect. C Struct. Chem. 71 (2015) 3–8, doi:10.1107/S2053229614024218.